DUKE-TH-
CMU–HEP95–10
DOE–ER/40682–100

Kaon-Nucleon Couplings for Weak Decays of Hypernuclei

Martin J. Savage
Department of Physics, Carnegie Mellon University, Pittsburgh, PA 15213
savage@thepub.phys.cmu.edu

Roxanne P. Springer
Duke University Department of Physics, Durham, NC 27708
rps@phy.duke.edu

Abstract

We investigate the weak kaon-nucleon (NNK) S-wave and P-wave interactions using heavy baryon chiral perturbation theory. The leading 1-loop SU(3) breaking contributions to the ppK, pnK, and nnK couplings are computed. We find that they suppress all NNK amplitudes by 30% to 50%. The ratio of neutron-induced to proton-induced hypernuclear decay widths is sensitive to such reductions. It has been argued that the discrepancy between the predicted and observed P-wave amplitudes in $\Delta s = 1$ hyperon decay results from an accidental cancellation between tree-level amplitudes, and is not a fundamental problem for chiral perturbation theory. Agreement between experimentally determined NNK P-wave amplitudes and our estimates would support this explanation.

I. INTRODUCTION

Weak decays of hypernuclei provide a laboratory for investigating kaon-nucleon interactions. In free space, a hyperon such as Λ, Σ or Ξ will decay predominantly through a mesonic mode, e.g. $\Lambda \to N\pi$. However, when the hyperon is bound inside a nucleus with $A \sim 12$ or larger, this decay mode is suppressed by Pauli-blocking of the final state nucleon (produced with $\vec{p}_N \sim 100$ MeV/c, much less than the Fermi-momentum $\vec{p}_F \sim 280$ MeV/c). A competing process that does not suffer significantly from Pauli-blocking is nonmesonic weak scattering, e.g. $\Lambda N \to NN$, in which the final state nucleons have $\vec{p}_N \sim 400$ MeV/c. These processes occur at low momentum scales where QCD is in the nonperturbative regime, so the structure and decays of Λ, Σ, and Ξ hypernuclei have been investigated using various phenomenological models, e.g. [1–13]. Available experimental observables for analyzing such systems include spin-averaged decay rates, the proton asymmetry from polarised hypernuclei, and the ratio of neutron induced to proton induced decay widths. The later proves especially difficult to describe using hadronic models, implying that we do not yet have a complete understanding of the dynamics of these systems.

The weak scattering process receives contributions from long distance meson exchange diagrams and from short distance (compared to the scale of chiral symmetry breaking, $\Lambda_\chi \sim 1$ GeV) four-baryon contact terms. The leading meson exchange graphs are the one-pion exchange (OPE) followed by one-kaon exchange (OKE), one-eta exchange (OEE) and two-pion exchange (TPE) and so forth. The OPE amplitudes can be determined relatively well because both the weak and strong vertices have been experimentally determined. The OKE and OEE graphs are expected to be the next largest contribution and model computations [9] show that a significant contribution ($\sim 30\%$) to the nonmesonic decay mode may come from the OKE amplitude. More importantly, it has been demonstrated that the ratio of neutron-induced to proton-induced decay widths of Λ hypernuclei is sensitive to the weak OKE amplitude [14], which, for the currently used values for the NNK vertices, significantly cancels the contribution of the OPE amplitude. The resulting small ratio found for ${}^{12}_{\Lambda}C$ [14] is not consistent with what is seen experimentally [15–17], although experimental uncertainties are large. It also appears that vector meson exchange (e.g. $K^*, \rho, ...$) contributes to this ratio [14]. Such exchanges would be included in local four-baryon $\Delta s = 1$ operators in chiral perturbation theory.

It is not possible to make a direct experimental determination of the NNK weak couplings that appear in the nonmesonic decay amplitudes; instead, flavour SU(3) is used to relate these couplings to the weak pion couplings. Previous analyses of hypernuclear decay have either ignored SU(3) breaking or assigned an arbitrary 30% uncertainty to these couplings as an estimate of the SU(3) breaking, eg. [12] . We will estimate the size of SU(3) breaking in the NNK amplitudes using chiral perturbation theory.

Understanding the NNK weak interactions may shed light on a troubling situation encountered in the decay of free hyperons outside the role they play in hypernuclear decay. Both the S-wave and P-wave amplitudes for $\Delta s = 1$ hyperon decay are well studied experimentally. The S-wave amplitudes are adequately described, even at tree-level, by a weak operator transforming as an $(8_L, 1_R)$ under chiral $\mathrm{SU(3)_L} \otimes \mathrm{SU(3)_R}$. A long standing problem is that the P-wave amplitudes are not well reproduced at tree-level using the coupling constants extracted from the S-wave amplitudes. A one-loop calculation of the leading SU(3)

corrections to hyperon decay, performed in ref. [19], showed that this situation is not improved by including the leading terms nonanalytic in the strange quark mass. Further, these corrections change the tree level prediction of P-wave amplitudes by 100% (typical SU(3) breaking corrections are $\sim$ 30%), causing concern [20,21] that chiral perturbation theory may not be valid for such processes. It was suggested in ref. [19] that the problem may instead be that the weak coupling constants extracted from S-wave fits lead to (accidental) cancellations between the tree-level P-wave amplitudes. Large SU(3) breaking effects are then a result of small tree-level amplitudes, and not a breakdown of chiral perturbation theory. Since there is only one graph that contributes to P-wave NNK interactions at tree-level, such accidental cancellations are absent. Experimental determination of these weak NNK vertices would provide an indication of the applicability of chiral perturbation theory to such processes.

II. THE CHIRAL LAGRANGIAN FOR NONLEPTONIC INTERACTIONS

At the momentum transfers characteristic of nonmesonic hypernuclear decay, $p < \Lambda_\chi$, the relevant degrees of freedom are the lowest mass octet and decuplet baryons and the pseudo-Goldstone bosons π, K, and η. The low energy strong interaction of the these hadrons is described by the Lagrange density

$$\begin{aligned}\mathcal{L}^{st} = & \, i\mathrm{Tr}\bar{B}_v\,(v\cdot\mathcal{D})\,B_v + 2D\ \mathrm{Tr}\bar{B}_v S_v^\mu\{A_\mu, B_v\} + 2F\ \mathrm{Tr}\bar{B}_v S_v^\mu[A_\mu, B_v] \\ & -i\bar{T}_v^\mu(v\cdot\mathcal{D})\ T_{v\mu} + \Delta m\bar{T}_v^\mu T_{v\mu} + \mathcal{C}\left(\bar{T}_v^\mu A_\mu B_v + \bar{B}_v A_\mu T_v^\mu\right) \\ & +2\mathcal{H}\ \bar{T}_v^\mu S_{v\nu} A^\nu T_{v\mu} + \frac{f^2}{8}\mathrm{Tr}\partial_\mu\Sigma\partial^\mu\Sigma^\dagger + \mu\mathrm{Tr}\left(m_q\Sigma + m_q^\dagger\Sigma^\dagger\right) \ + \ \cdots \quad , \end{aligned} \tag{2.1}$$

where f is the meson decay constant, m_q is the light quark mass matrix, $\mathcal{D}_\mu = \partial_\mu + [V_\mu,\ ]$ is the covariant chiral derivative and use is made of the vector and axial vector chiral currents

$$\begin{aligned} V_\mu &= \frac{1}{2}(\xi\partial_\mu\xi^\dagger + \xi^\dagger\partial_\mu\xi) \\ A_\mu &= \frac{i}{2}(\xi\partial_\mu\xi^\dagger - \xi^\dagger\partial_\mu\xi) \quad . \end{aligned} \tag{2.2}$$

The dots in Eq. (2.1) represent higher dimension operators (involving more derivatives and insertions of the light quark mass matrix) whose contributions are suppressed by inverse powers of Λ_χ. The octet baryon field of four-velocity v is denoted by B_v and has SU(3) elements

$$B_v = \begin{pmatrix} \frac{1}{\sqrt{2}}\Sigma_v^0 + \frac{1}{\sqrt{6}}\Lambda_v & \Sigma_v^+ & p_v \\ \Sigma_v^- & -\frac{1}{\sqrt{2}}\Sigma_v^0 + \frac{1}{\sqrt{6}}\Lambda_v & n_v \\ \Xi_v^- & \Xi_v^0 & -\frac{2}{\sqrt{6}}\Lambda_v \end{pmatrix} \quad , \tag{2.3}$$

and the decuplet baryons appear as the elements of the (totally symmetric) T_v:

$$T_v^{111} = \Delta_v^{++}, \quad T_v^{112} = \frac{1}{\sqrt{3}}\Delta_v^+, \quad T_v^{122} = \frac{1}{\sqrt{3}}\Delta_v^0, \quad T_v^{222} = \Delta_v^-,$$

$$T_v^{113} = \frac{1}{\sqrt{3}}\Sigma_v^{*+}, \quad T_v^{123} = \frac{1}{\sqrt{6}}\Sigma_v^{*0}, \quad T_v^{223} = \frac{1}{\sqrt{3}}\Sigma_v^{*-}, \quad T_v^{133} = \frac{1}{\sqrt{3}}\Xi_v^{*0},$$
$$T_v^{233} = \frac{1}{\sqrt{3}}\Xi_v^{*-}, \quad T_v^{333} = \Omega_v^- \quad . \tag{2.4}$$

The octet of pseudoscalar pseudo-Goldstone bosons resulting from the spontaneous breaking of chiral symmetry appear in the Σ field, with

$$\Sigma = \xi^2 = \exp\left(\frac{2iM}{f}\right) \quad , \tag{2.5}$$

where

$$M = \begin{pmatrix} \frac{1}{\sqrt{6}}\eta + \frac{1}{\sqrt{2}}\pi^0 & \pi^+ & K^+ \\ \pi^- & \frac{1}{\sqrt{6}}\eta - \frac{1}{\sqrt{2}}\pi^0 & K^0 \\ K^- & \overline{K}^0 & -\frac{2}{\sqrt{6}}\eta \end{pmatrix} \quad . \tag{2.6}$$

The strong couplings constants $F, D, \mathcal{C}$ and $\mathcal{H}$ have been determined from one-loop computations of axial matrix elements between octet baryons [18] and strong decays of decuplet baryons [22].

The $\Delta s = 1$ weak interactions of the pseudo-Goldstone bosons and the lowest lying baryons are described, assuming octet dominance, by the Lagrange density

$$\begin{aligned} \mathcal{L}_v^{\Delta s=1} &= G_F m_\pi^2 f_\pi h_D \mathrm{Tr}\overline{B}_v\{\xi^\dagger h \xi\,, B_v\} \;+\; G_F m_\pi^2 f_\pi h_F \mathrm{Tr}\overline{B}_v[\xi^\dagger h \xi\,, B_v] \\ &+ G_F m_\pi^2 f_\pi h_C \overline{T}_v^\mu (\xi^\dagger h \xi) T_{v\mu} \;+\; G_F m_\pi^2 h_\pi \frac{f_\pi^2}{8}\mathrm{Tr}\left(h\,\partial_\mu \Sigma \partial^\mu \Sigma^\dagger\right) \;+\; \cdots \quad , \end{aligned} \tag{2.7}$$

where

$$h = \begin{pmatrix} 0 & 0 & 0 \\ 0 & 0 & 1 \\ 0 & 0 & 0 \end{pmatrix} \quad , \tag{2.8}$$

and the constants f_π, h_D, h_F, h_π and h_C are determined experimentally. The pion decay constant is known to be $f_\pi \sim 132$ MeV. We have inserted factors of $G_F m_\pi^2 f_\pi$ in Eq. (2.7) so that the constants h_D, h_F, h_π and h_C are dimensionless and of order unity. At tree-level, the weak decay of the octet baryons gives [18,19] $h_D = -0.58$ and $h_F = +1.40$, while the weak decay of the Ω^- gives $h_C \sim 1.4$. The weak meson coupling h_π is determine from nonleptonic kaon decays to be $h_\pi = 1.4$. The dots denote higher dimension operators involving more derivatives and insertions of the light quark mass matrix.

We will determine the S-wave and P-wave amplitudes for weak NNK interactions, including the SU(3) violating one-loop corrections. In the spirit of chiral perturbation theory we compute the leading nonanalytic corrections dependent upon the mass of the strange quark, of the form $m_s \log m_s$. This requires the computation of one-loop graphs involving kaons, pions, and etas with octet and/or decuplet baryons. Such graphs are divergent and regularized in n-dimensions with modified minimal subtraction, $\overline{MS}$. The divergences are absorbed by higher dimension operators whose coefficients depend upon the renormalization scale. The sum of the counterterm and the loop graph is scale independent. By choosing to

renormalize at the chiral symmetry breaking scale, and using the fact that the coefficients of the higher dimension operators are analytic functions of the light quarks masses, the size of these coefficients can be *estimated* using naive dimensional analysis. In the chiral limit the contributions from the higher dimension operators are subdominant compared to the logarithms that arise from the loop graphs involving the lowest dimension operators. It is these chiral logarithms that we compute in this work. For physical values of the kaon, pion, and eta masses, these quantities represent only an estimate of the size of SU(3) breaking effects; contributions from local counterterms will be of the same order. Unfortunately, the coefficients of the counterterms are not directly computable from the chiral Lagrangian and must be determined experimentally.

The amplitude for the weak $\Delta s = 1$ NNK interactions has the form

$$\mathcal{A} = iG_F m_\pi^2 \, \frac{f_\pi}{f_K} \, \overline{N}_v \, \left[\mathcal{A}^{(S)} + 2\frac{k \cdot S_v}{\Lambda_\chi} \mathcal{A}^{(P)} \right] N_v \tag{2.9}$$

where N_v contains the nucleon doublet

$$N_v = \begin{pmatrix} p_v \\ n_v \end{pmatrix} \quad , \tag{2.10}$$

and k is the outgoing momentum of the kaon. The amplitudes $\mathcal{A}^{(S)}$ and $\mathcal{A}^{(P)}$ are the S-wave and P-wave amplitudes respectively, and are computed below. We have chosen to normalize $\mathcal{A}^{(P)}$ to Λ_χ so that it is dimensionless. An explicit factor of f_π/f_K appears in Eq. (2.9) and further we will distinguish f_K from f_π in the expressions arising from the one loop amplitudes. There is evidence from other loop computations that this SU(3) breaking difference should be included explicitly [23].

III. COMPUTATION OF AMPLITUDES

There are three vertices that occur in $\Delta s = 1$ weak nonleptonic interactions involving nucleons and kaons: $p\bar{p}K^0$, $n\bar{p}K^+$, and $n\bar{n}K^0$. They are not independent in the limit of isospin symmetry and are related by

$$\mathcal{A}^{(L)}(nnK) - \mathcal{A}^{(L)}(ppK) = \mathcal{A}^{(L)}(npK) \quad , \tag{3.1}$$

where $L = 0$ (S-wave) or $L = 1$ (P-wave); this relation is true for both S-wave and P-wave amplitudes independently. The amplitudes

$$\mathcal{A}^{(L)} = \mathcal{A}_0^{(L)} + \mathcal{A}_1^{(L)} + \cdots \ , \tag{3.2}$$

where the subscript denotes the order in chiral perturbation theory and the dots indicate contributions arising from more insertions of the light quark mass matrix or involving more derivatives.

A. S-Wave Amplitudes

At tree level (see Fig. 1) the S-wave amplitudes appear directly from the first and second terms in the weak Lagrangian of Eq. (2.7) ,

$$\begin{aligned}\mathcal{A}_0^{(S)}(p\bar{p}K^0) &= h_F - h_D \\ \mathcal{A}_0^{(S)}(p\bar{n}K^+) &= h_F + h_D \\ \mathcal{A}_0^{(S)}(n\bar{n}K^0) &= 2h_F \quad .\end{aligned} \tag{3.3}$$

Using experimental measurements of hyperon decay to fix h_D and h_F, these amplitudes are 2.0, 0.8, and 2.8, respectively. They will be modified by SU(3) breaking effects since their tree-level values are determined by pionic hyperon decay and the amplitudes in question involve kaons and nucleons. Direct computation of the loop graphs shown in Fig. 2 lead to S-wave amplitudes

$$\begin{aligned}\mathcal{A}_1^{(S)}(p\bar{p}K^0) = \frac{m_K^2}{16\pi^2 f_K^2}\log\left(\frac{m_K^2}{\Lambda_\chi^2}\right)\Big(&\frac{h_D}{3}(1+13D^2-18DF-27F^2) \\ &+\frac{h_F}{3}(-7-7D^2+6DF+9F^2)\Big) \\ +\frac{2C^2}{9}h_C\mathcal{J}(\Delta m_N^{\Sigma^*}) &- \mathcal{A}_0^{(S)}(p\bar{p}K^0)\mathcal{Z}_\Psi \quad ,\end{aligned} \tag{3.4}$$

$$\begin{aligned}\mathcal{A}_1^{(S)}(p\bar{n}K^+) = \frac{m_K^2}{16\pi^2 f_K^2}\log\left(\frac{m_K^2}{\Lambda_\chi^2}\right)\Big(&\frac{h_D}{3}(2-4D^2-24F+36F^2) \\ &+\frac{h_F}{3}(2+20D^2-48DF+36F^2)\Big) \\ -\frac{4C^2}{9}h_C\mathcal{J}(\Delta m_N^{\Sigma^*}) &- \mathcal{A}_0^{(S)}(p\bar{n}K^+)\mathcal{Z}_\Psi \quad ,\end{aligned} \tag{3.5}$$

$$\begin{aligned}\mathcal{A}_1^{(S)}(n\bar{n}K^0) = \frac{m_K^2}{16\pi^2 f_K^2}\log\left(\frac{m_K^2}{\Lambda_\chi^2}\right)\Big(&h_D(1+3D^2-14DF+3F^2) \\ &+\frac{h_F}{3}(-5+13D^2-42DF+45F^2)\Big) \\ -\frac{2}{9}C^2h_C\mathcal{J}(\Delta m_N^{\Sigma^*}) &- \mathcal{A}_0^{(S)}(n\bar{n}K^0)\mathcal{Z}_\Psi \quad ,\end{aligned} \tag{3.6}$$

where the contribution from wavefunction renormalization is given by

$$\mathcal{Z}_\Psi = \frac{m_K^2}{16\pi^2 f_K^2}\log(\frac{m_K^2}{\Lambda_\chi^2})\Big(15F^2-10FD+\frac{17}{3}D^2\Big) + C^2\mathcal{J}(\Delta m_N^{\Sigma^*}) \quad , \tag{3.7}$$

and the function $\mathcal{J}$ is

$$\mathcal{J}(\delta) = \frac{1}{16\pi^2 f_K^2}\left[(m_K^2-2\delta^2)\log\left(\frac{m_K^2}{\Lambda_\chi^2}\right) + 2\delta\sqrt{\delta^2-m_K^2}\log\left(\frac{\delta-\sqrt{\delta^2-m_K^2+i\epsilon}}{\delta+\sqrt{\delta^2-m_K^2+i\epsilon}}\right)\right] \quad . \tag{3.8}$$

For S-waves, $\delta = \Delta m_N^{\Sigma^*} = m_{\Sigma^*} - m_N$. The kaon decay constant $f_K = 1.22\ f_\pi$.

We have not included wavefunction renormalization of the external meson field in our KNN amplitude computations since the kaons do not appear as asymptotic states in the weak scattering processes under consideration.

In order to determine the $\mathcal{A}^{(S)}$ we insert the axial coupling constants $D, F, \mathcal{C}$, and $\mathcal{H}$ extracted by the one-loop computations of [18,22]:

$$\begin{aligned} D &= 0.6 \pm 0.1 \quad , \quad F = 0.4 \pm 0.1 \\ \mathcal{C} &= -1.2 \pm 0.1 \quad , \quad \mathcal{H} = -2.0 \pm 0.2 \quad , \end{aligned} \tag{3.9}$$

and the weak coupling constants determined at one-loop level [19]

$$\begin{aligned} h_D &= -0.35 \pm 0.09 \quad , \quad h_F = 0.86 \pm 0.05 \\ h_C &= -0.36 \pm 0.65 \quad . \end{aligned} \tag{3.10}$$

The uncertainties in these couplings are treated as uncorrelated for the purpose of determining the uncertainty in the NNK amplitudes. We determine the error in the NNK amplitudes by varying the parameters over their allowed range and require that the choice of parameters reproduce the $\Delta s = 1$ S-wave hyperon amplitudes within their uncertainties. In this way we determine that, with $\Lambda_\chi = 1$ GeV,

$$\begin{aligned} \mathcal{A}_0^{(S)}(p\bar{p}K^0) + \mathcal{A}_1^{(S)}(p\bar{p}K^0) &= 1.5 \pm 0.1 \\ \mathcal{A}_0^{(S)}(p\bar{n}K^+) + \mathcal{A}_1^{(S)}(p\bar{n}K^+) &= 0.4 \pm 0.1 \\ \mathcal{A}_0^{(S)}(n\bar{n}K^0) + \mathcal{A}_1^{(S)}(n\bar{n}K^0) &= 1.9 \pm 0.1 \end{aligned} \tag{3.11}$$

The SU(3) corrections tend to suppress the couplings compared to their tree-level values, a significant contribution of which comes from the use of the one-loop extracted weak couplings in the tree-level amplitudes instead of those extracted at tree-level. The corrections to the ppK and nnK couplings are, as one expects for SU(3) breaking, at the 30% level. However, the corrections to the pnK amplitude lead to an effective coupling approximately half the strength computed at tree-level.

B. P-Waves

The tree level P-wave amplitudes come directly from pole graphs involving one weak vertex from Eq. (2.7) and one strong vertex from Eq. (2.1), (see Fig. 1)

$$\begin{aligned} \frac{\mathcal{A}_0^{(P)}(p\bar{p}K^0)}{\Lambda_\chi} &= -\frac{(D-F)(h_D - h_F)}{m_N - m_\Sigma} \\ \frac{\mathcal{A}_0^{(P)}(p\bar{n}K^+)}{\Lambda_\chi} &= -\frac{1}{6}\frac{(D+3F)(h_D+3h_F)}{m_N - m_\Lambda} + \frac{1}{2}\frac{(D-F)(h_D-h_F)}{m_N - m_\Sigma} \\ \frac{\mathcal{A}_0^{(P)}(n\bar{n}K^0)}{\Lambda_\chi} &= -\frac{1}{6}\frac{(D+3F)(h_D+3h_F)}{m_N - m_\Lambda} - \frac{1}{2}\frac{(D-F)(h_D-h_F)}{m_N - m_\Sigma} \quad . \end{aligned} \tag{3.12}$$

Using the experimentally determined values of the parameters D, F, h_D, and h_F (Eq. (3.9) and Eq. (3.10)), the values for these tree level amplitudes become –4.8, 18, and 13 ($\times\Lambda_\chi/1\,\mathrm{GeV}$), respectively. Loop diagrams as shown in Fig. 3 then give

$$\begin{aligned}
\frac{\mathcal{A}_1^{(P)}(p\bar{p}K^0)}{\Lambda_\chi} = \frac{m_K^2}{16\pi^2 f_K^2}\log\left(\frac{m_K^2}{\Lambda_\chi^2}\right)\times
&\left[\frac{h_D}{m_N-m_\Sigma}\left[\frac{10}{3}D-\frac{10}{3}F+\frac{92}{9}D^3-\frac{140}{9}D^2F+\frac{20}{3}DF^2-4F^3\right]\right.\\
&+\frac{h_F}{m_N-m_\Sigma}\left[\frac{10}{3}F-\frac{10}{3}D-\frac{56}{9}D^3+\frac{140}{9}D^2F-\frac{32}{3}DF^2+4F^3\right]\\
&\left.+h_\pi\left[\frac{5}{36}D+\frac{7}{36}F-\frac{2}{9}D^3+\frac{1}{9}D^2F+\frac{28}{9}DF^2-\frac{1}{3}F^3\right]\right]\\
&-\frac{10}{81}C^2\mathcal{H}\frac{h_D-h_F}{m_N-m_\Sigma}\mathcal{J}(\Delta m_N^{\Sigma^*})-\frac{2}{9}\frac{D-F}{m_N-m_\Sigma}C^2h_C\mathcal{J}(\Delta m_N^{\Sigma^*})\\
&-\frac{2}{9}C^2\frac{h_D-h_F}{m_N-m_\Sigma}[(D+5F)\mathcal{K}(m_K,\Delta m_N^{\Sigma^*})-(D-3F)\mathcal{K}(m_\eta,\Delta m_N^{\Sigma^*})]\\
&+\frac{10}{81}h_\pi C^2\mathcal{H}\mathcal{J}(\Delta m_N^{\Delta})\\
&+h_\pi C^2\Big[\frac{4}{9}(D-F)\mathcal{K}(m_K,\Delta m_N^{\Delta})+\frac{2}{9}(F+D)\mathcal{K}(m_K,\Delta m_N^{\Sigma^*})\\
&\qquad\qquad-\frac{1}{27}(D-3F)G_{\eta K\Sigma^*}\Big]\\
&+\frac{(D-F)(h_D-h_F)}{m_N-m_\Sigma}\frac{14}{3}C^2\mathcal{J}(\Delta m_\Sigma)-\mathcal{A}_0^{(P)}(p\bar{p}K^0)\mathcal{Z}_\Psi\quad,
\end{aligned}\tag{3.13}$$

where $\mathcal{Z}_\Psi$ is the same wavefunction renormalization employed for the S-wave expressions.

$$\begin{aligned}
\frac{\mathcal{A}_1^{(P)}(p\bar{n}K^+)}{\Lambda_\chi} = \frac{m_K^2}{16\pi^2 f_K^2}\log(\frac{m_K^2}{\Lambda_\chi^2})\Big(&\frac{h_D}{m_N-m_\Lambda}\Big[\frac{5}{9}D+\frac{5}{3}F+\frac{2}{27}D^3+2D^2F+\frac{34}{3}DF^2+6F^3\Big]\\
&+\frac{h_F}{m_N-m_\Lambda}\Big[\frac{5}{3}D+5F+\frac{20}{9}D^3+6D^2F+16DF^2+18F^3\Big]\\
&+\frac{h_D}{m_N-m_\Sigma}\Big[-\frac{5}{3}D+\frac{5}{3}F-\frac{46}{9}D^3+\frac{70}{9}D^2F-\frac{10}{3}DF^2+2F^3\Big]\\
&+\frac{h_F}{m_N-m_\Sigma}\Big[\frac{5}{3}D-\frac{5}{3}F+\frac{28}{9}D^3-\frac{70}{9}D^2F+\frac{16}{3}DF^2-2F^3\Big]\\
&-h_\pi\Big[\frac{11}{36}D+\frac{11}{36}F-\frac{14}{27}D^3+\frac{1}{3}D^2F+\frac{20}{9}DF^2+\frac{1}{3}F^3\Big]\Big)\\
+\frac{5}{9}C^2\mathcal{H}\mathcal{J}(\Delta m_N^{\Sigma^*})&\Big[\frac{1}{3}\frac{h_D+3h_F}{m_N-m_\Lambda}+\frac{1}{9}\frac{h_D-h_F}{m_N-m_\Sigma}\Big]\\
+C^2\Big[\Big(&-\frac{1}{3}\frac{(h_D+3h_F)(D+F)}{m_N-m_\Lambda}+\frac{1}{9}\frac{(h_D-h_F)(D+5F)}{m_N-m_\Sigma}\Big)\mathcal{K}(m_K,\Delta m_N^{\Sigma^*})\\
&-\frac{1}{9}\frac{(h_D-h_F)(D-3F)}{m_N-m_\Sigma}\mathcal{K}(m_\eta,\Delta m_N^{\Sigma^*})\Big]\\
+C^2h_C\mathcal{J}(\Delta m_N^{\Sigma^*})&\Big[\frac{1}{9}\frac{D-F}{m_N-m_\Sigma}+\frac{1}{3}\frac{D+3F}{m_N-m_\Lambda}\Big]+\frac{10}{81}h_\pi C^2\mathcal{H}\mathcal{J}(\Delta m_N^{\Sigma^*})
\end{aligned}$$

$$
\begin{aligned}
&+ h_\pi C^2\Big[\frac{4}{9}(D-F)\mathcal{K}(m_K,\Delta m_N^{\Delta}) - \frac{5}{18}(F+D)\mathcal{K}(m_K,\Delta m_N^{\Sigma^*}) \\
&\qquad\qquad - \frac{1}{54}(D-3F)G_{\eta K\Sigma^*}\Big] \\
&+ C^2\Big[\frac{1}{3}\frac{(h_D+3h_F)}{m_N-m_\Lambda}(D+3F) - \frac{7}{3}\frac{h_D-h_F}{m_N-m_\Sigma}(D-F)\Big]\mathcal{J}(\Delta m_\Sigma) \\
&- \mathcal{A}_0^{(P)}(n\bar{p}K^+)\mathcal{Z}_\Psi \quad , \qquad (3.14)
\end{aligned}
$$

$$
\begin{aligned}
\frac{\mathcal{A}_1^{(P)}(n\bar{n}K^0)}{\Lambda_\chi} = {}& \frac{m_K^2}{16\pi^2 f_K^2}\log(\frac{m_K^2}{\Lambda_\chi^2})\Big(\frac{h_D}{m_N-m_\Lambda}\Big[\frac{5}{9}D+\frac{5}{3}F+\frac{2}{27}D^3+2D^2F+\frac{34}{3}DF^2+6F^3\Big] \\
&+\frac{h_F}{m_N-m_\Lambda}\Big[\frac{5}{3}D+5F+\frac{20}{9}D^3+6D^2F+16DF^2+18F^3\Big] \\
&+\frac{h_D}{m_N-m_\Sigma}\Big[\frac{5}{3}D-\frac{5}{3}F+\frac{46}{9}D^3-\frac{70}{9}D^2F+\frac{10}{3}DF^2-2F^3\Big] \\
&+\frac{h_F}{m_N-m_\Sigma}\Big[-\frac{5}{3}D+\frac{5}{3}F-\frac{28}{9}D^3+\frac{70}{9}D^2F-\frac{16}{3}DF^2+2F^3\Big] \\
&-h_\pi\Big[\frac{3}{18}D+\frac{1}{9}F-\frac{8}{27}D^3+\frac{2}{9}D^2F-\frac{8}{9}DF^2+\frac{2}{3}F^3\Big] \\
&+\frac{5}{9}C^2\mathcal{H}\mathcal{J}(\Delta m_N^{\Sigma^*})\Big[\frac{1}{3}\frac{h_D+3h_F}{m_N-m_\Lambda}-\frac{1}{9}\frac{h_D-h_F}{m_N-m_\Sigma}\Big] \\
&+C^2\Big[\Big(-\frac{1}{9}\frac{(h_D-h_F)(D+5F)}{m_N-m_\Sigma}-\frac{1}{3}\frac{(h_D+3h_F)(D+F)}{m_N-m_\Lambda}\Big)\mathcal{K}(m_K,\Delta m_N^{\Sigma^*}) \\
&\qquad+\Big(\frac{1}{9}\frac{(h_D-h_F)(D-3F)}{m_N-m_\Sigma}\Big)\mathcal{K}(m_\eta,\Delta m_N^{\Sigma^*})\Big] \\
&-C^2h_C\,\mathcal{J}(\Delta m_N^{\Sigma^*})\Big[\frac{1}{9}\frac{D-F}{m_N-m_\Sigma}-\frac{1}{3}\frac{D+3F}{m_N-m_\Lambda}\Big]+\frac{20}{81}h_\pi C^2\mathcal{H}\mathcal{J}(\Delta m_N^{\Delta}) \\
&+h_\pi C^2\Big[\frac{8}{9}(D-F)\mathcal{K}(m_K,\Delta_N^{\Delta})-\frac{1}{18}(F+D)\mathcal{K}(m_K,\Delta_N^{\Sigma^*}) \\
&\qquad\qquad-\frac{1}{54}(D-3F)G_{\eta K\Sigma^*}\Big] \\
&+C^2\Big[\frac{1}{3}\frac{h_D+3h_F}{m_N-m_\Lambda}(D+3F)+\frac{7}{3}\frac{h_D-h_F}{m_N-m_\Sigma}(D-F)\Big]\mathcal{J}(\Delta m_\Sigma) \\
&-\mathcal{A}_0^{(P)}(n\bar{n}K^0)\mathcal{Z}_\Psi \quad . \qquad (3.15)
\end{aligned}
$$

The function $\mathcal{K}(m,\Delta)$ which appears in Eq. (3.13), Eq. (3.14) and Eq. (3.15) from diagrams having both decuplet and octet intermediate states is

$$
\begin{aligned}
\mathcal{K}(m,\delta) = {}& \frac{1}{16\pi^2 f_K^2}\Big\{(m^2-\frac{2}{3}\delta^2)\log(\frac{m^2}{\Lambda_\chi^2}) \\
&+\frac{2}{3}\frac{1}{\delta}\Big[(\delta^2-m^2)^{3/2}\log\left(\frac{\delta-\sqrt{\delta^2-m^2+i\epsilon}}{\delta+\sqrt{\delta^2-m^2+i\epsilon}}\right)+\pi m^3\Big]\Big\} \quad , \qquad (3.16)
\end{aligned}
$$

and the function $G_{m_1,m_2,B}$ is given by

$$G_{m_1,m_2,B} = \frac{m_1^2}{m_1^2 - m_2^2}\mathcal{K}(m_1, \Delta_N^B) + \frac{m_2^2}{m_2^2 - m_1^2}\mathcal{K}(m_2, \Delta_N^B) \quad . \tag{3.17}$$

The mass differences that appear in Eq. (3.13), Eq. (3.14) and Eq. (3.15) are defined by

$$\begin{aligned} \Delta m_N^{\Sigma^*} &= m_\Sigma^* - m_N \quad , \quad \Delta m_N^\Delta = m_\Delta - m_N \\ \Delta m_\Sigma &= m_{\Xi^*} - m_\Sigma \ \sim \ \Delta m_N^{\Sigma^*} \quad . \end{aligned} \tag{3.18}$$

In the same way that the S-wave KNN amplitudes and associated uncertainties were determined, we use the expressions for S-wave hyperon decay [19], along with experimental measurements, to generate P-wave KNN amplitudes consistent with S-wave hyperon decay rates. The results, with $\Lambda_\chi = 1$ GeV, are

$$\begin{aligned} \mathcal{A}_0^{(P)}(p\bar{p}K^+) + \mathcal{A}_1^{(P)}(p\bar{p}K^+) &= -3.2 \pm 0.3 \\ \mathcal{A}_0^{(P)}(p\bar{n}K^+) + \mathcal{A}_1^{(P)}(p\bar{n}K^+) &= 14 \pm 1 \\ \mathcal{A}_0^{(P)}(n\bar{n}K^+) + \mathcal{A}_1^{(P)}(n\bar{n}K^+) &= 11 \pm 1 \end{aligned} \tag{3.19}$$

The P-wave amplitudes are seen to be reduced by $\sim 30\%$ from their tree-level values by the SU(3) breaking one-loop contributions. This is in contrast to the $\Delta s = 1$ hyperon decay P-wave amplitudes, where the corrections are at the 100% level. The NNK SU(3) breaking is the size one would naively guess and is consistent with the idea [19] that the large corrections to the P-wave amplitudes for $\Delta s = 1$ hyperon decays are the result of accidentally small tree level amplitudes, and not a breakdown of chiral perturbation theory.

IV. DISCUSSION

Weak NNK amplitudes that contribute to nonmesonic hypernuclear decay are not directly measurable but can be related to $\Delta s = 1$ hyperon decay by flavour SU(3). We have computed the leading SU(3) breaking contributions to these amplitudes using heavy baryon chiral perturbation theory and find that such corrections suppress both the S-wave and P-wave amplitudes by 30% to 50%.

	S-waves		*P-waves*	
vertex	$\mathcal{A}_0^{(S)}$	$\mathcal{A}_0^{(S)} + \mathcal{A}_1^{(S)}$	$\mathcal{A}_0^{(P)}$	$\mathcal{A}_0^{(P)} + \mathcal{A}_1^{(P)}$
$p\overline{p}K^0$	2.0	1.5 ± 0.1	-4.8	-3.2 ± 0.3
$p\overline{n}K^+$	0.8	0.4 ± 0.1	18	14 ± 1
$n\overline{n}K^0$	2.8	1.9 ± 0.1	13	11 ± 1

Table 1. The S-wave and P-wave amplitudes at tree-level and one-loop. We have set $\Lambda_\chi = 1$ GeV in both the S-wave and P-wave amplitudes.

In $\Delta s = 1$ mesonic hyperon decay there are two tree-level graphs contributing to P-wave amplitudes which tend to cancel against each other for the values of weak couplings constants determined from S-wave hyperon decay amplitudes. Since there is only one graph contributing to the P-wave NNK vertices, no such cancellations arise and the amplitudes are, in general, less susceptible to large SU(3) violation. It would be interesting to compare the P-wave amplitudes extracted from hypernuclear decay with the amplitudes computed in this work. It would help us to determine if the disagreement between the observed and predicted $\Delta s = 1$ mesonic hyperon decay P-wave amplitudes is an accident of nature or a hint that chiral perturbation theory is not applicable to these processes.

We stress that our computation is only an estimate of SU(3) breaking effects as there are unknown counterterms that also contribute. The computation that we have performed is the leading effect in the chiral limit, $m_q \to 0$. There is no reason to suspect that the counterterms cancel the loop contributions since the counterterms arise from UV physics whereas the nonanalytic terms from the loop graphs are IR effects.

In order to determine the impact of our work on the understanding of hypernuclear decay the NNK amplitudes, including the SU(3) breaking corrections, must be incorporated into a realistic hypernucleus in the same way that previous estimates of interaction strengths have been included, e.g. [9]. It seems likely that the results found in this work will have significant impact on theoretical predictions for the ratio of neutron-induced to proton-induced decay widths of Λ-hypernuclei, eg. ${}^{12}_{\Lambda}C$ [14], and possibly other flavours of hypernuclei.

V. ACKNOWLEDGEMENTS

We would like to thank the Institute for Nuclear Theory at the University of Washington for their kind hospitality during some of this work. RPS would also like to thank the Institute for Theoretical Physics at the University of California, Santa Barbara, and Carnegie-Mellon University, where some of this work was completed. MJS would like to thank Duke University where some of this work was carried out. MJS would also like to thank L. Kisslinger and C. Bennhold for useful discussions. Our work is supported in part by the US Dept. of Energy under grant number DE-FG02-91-ER40682, and grant number DE-FG05-90ER40592.

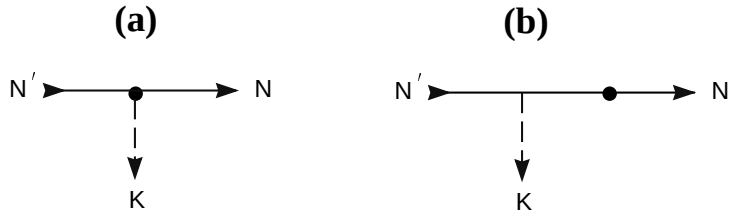

FIG. 1. Tree-level diagrams for the KNN amplitudes. (a) is the s-wave diagram, and (b) is the p-wave diagram. The dashed lines are mesons, and the solid lines are octet baryons. The unmarked vertex is a strong interaction and the black dots are weak vertices.

REFERENCES

[1] B.H.J. McKellar and B.F. Gibson, Phys. Rev C30 (1984) 322.
[2] J.F. Dubach, Nucl. Phys. A450 (1986) 71c.
[3] E. Oset and L.L. Salcedo, Nucl. Phys. A443 (1985) 704; A450 (1986) 371c.
[4] C-Y Cheung, D.P. Heddle and L.S. Kisslinger, Phys. Rev. C27 (1983) 335.
[5] D.P Heddle and L.S. Kisslinger, Phys. Rev. C33 (1986) 608.
[6] G. Nardulli, Phys. Rev. C38 (1988) 832.
[7] D.J. Millener, C.B. Dover and A. Gal, Phys. Rev. C38 (1988) 2700.
[8] J. Cohen, Prog. Part. Nucl. Phys. 25 (1990) 139.
[9] A. Ramos et al., Nucl. Phys. A544 (1992) 703.
[10] C. Dover, Nucl. Phys. A547 (1992) 27c.
[11] T. Inoue, S. Takeuchi, M. Oka, Nucl. Phys. A577 (1994) 281c.
[12] K. Maltman and M. Shmatikov, Phys. Lett. B331 (1994) 1.
[13] J. Mares and B.K. Jennings, Nucl. Phys. A585 (1995) 347c.
[14] C. Bennhold, presented at the Institute for Nuclear Theory, Seattle , Washington, August 1995.
[15] J. J. Szymanski, et al., Phys. Rev. C43 (1991) 849.
[16] S. Ajimura et al., Phys. Lett. B282 (1992) 293.
[17] H. Ejiri et al., presented at the conference on the "Intersections Between Particle and Nuclear Physics", p616, AIP Press (1995).
[18] E. Jenkins and A. Manohar, Phys. Lett. B255 (1991) 558; B259 (1991) 353.
[19] E. Jenkins, Nucl. Phys. B375 (1992) 561.
[20] J. Bijnens, H. Sonoda and M.B. Wise, Nucl. Phys. B261 (1985) 185.
[21] C. Carone and H. Georgi, Nucl. Phys. B375 (1992) 243.
[22] M.N. Butler, M.J. Savage and R.P. Springer, Nucl. Phys. B399 (1993) 69.
[23] E. Jenkins, M. Luke, A.V. Manohar and M.J. Savage, Phys. Letts. B302 (1993) 482.

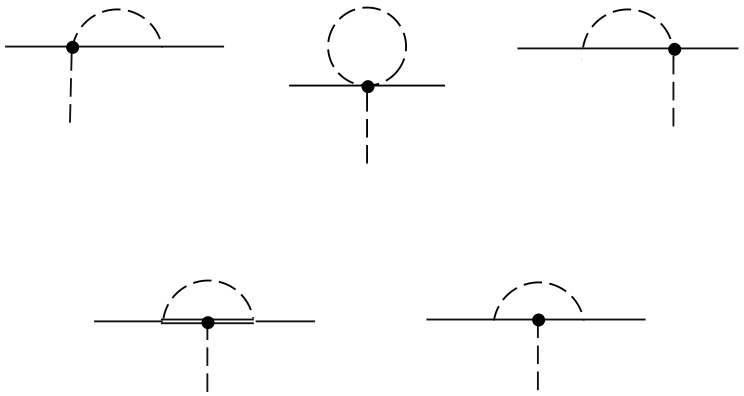

FIG. 2. One-loop graphs contributing to S-wave KNN amplitudes. Dashed lines are mesons, solid lines are octet baryons, and the double line indicates a decuplet baryon. The unmarked vertices are strong interactions. The black dot indicates a weak vertex.

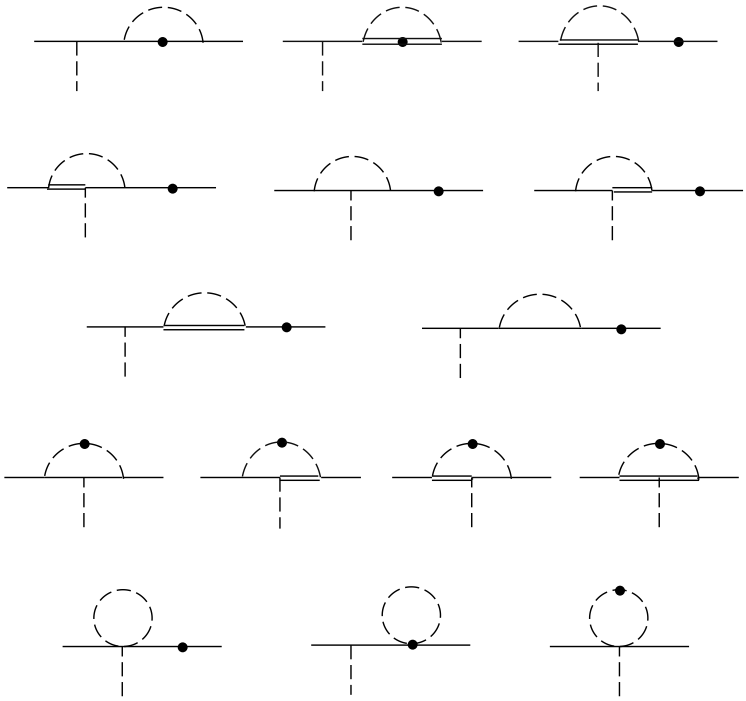

FIG. 3. One-loop graphs contributing to P-wave KNN amplitudes. Dashed lines are mesons, solid lines are octet baryons, and the double line indicates a decuplet baryon. The unmarked vertices are strong interactions. The black dot indicates a weak vertex.